Science in One Health 1 (2022) 100002

Contents lists available at ScienceDirect

Science in One Health

journal homepage: www.journals.elsevier.com/science-in-one-health

Review

Low temperature catalytic conversion of carbon monoxide by the application of novel perovskite catalysts

Subhashish Dey [a,*], Niraj Singh Mehta [b]

[a] Environmental Engineering Department, Rajiv Gandhi Proudyogiki Vishwavidyalaya, Bhopal, India
[b] Electronics and Communication Engineering, Krishna Institute of Engineering and Technology, Ghaziabad, Uttar Pradesh, India

ARTICLE INFO

Keywords:
Carbon monoxide
Catalyst
Perovskite
Electrically active structure and automobile

ABSTRACT

Automobile exhaust contributes the largest sources of carbon monoxide (CO) into the environment. To control this CO pollution, the catalytic converters have been discovered. The catalytic converters have been invented for regulating the CO discharge. There are many types of catalysts have been investigated for CO emission control purposes. Inorganic perovskite-type oxides are fascinating nanomaterials for wide applications in catalysis, fuel cells, and electrochemical sensing. Perovskites prepared in the nanoscale have recently received more attention due to their catalytic nature when used as electrode modifiers. Perovskite catalysts show great potential for CO oxidation catalyst in a catalytic converter for their low cost, high thermal stability and tailoring flexibility. It is active for CO oxidation at a lower temperature. The catalytic activity of these oxides is higher than that of many transition metals compounds and even some precious metal oxides. They represents attractive physical and chemical characteristics such as electronic conductivity, electrically active structure, the oxide ions mobility through the crystal lattice, variations on the content of the oxygen, thermal and chemical stability, and super-magnetic, photocatalytic, thermoelectric and dielectric properties. The surface sites and lattice oxygen species present in perovskite catalysts play an important role in chemical transformations. The partial replacement of cations A and B by different elements, which changes the atomic distance, causes unit cell disturbances, stabilizes various oxidation states or added cationic or anionic vacancies inside the lattice. The novel things disturb the solid reactivity by varying the reaction mechanism on the catalyst surface. Thus, the better cations replacement may represent more activity. There are lots of papers available to CO oxidation over perovskite catalysts but no review paper available in the literature that is represented to CO oxidation.

1. Introduction

Perovskite catalyst general formula ABO_3; typically the A elements are rare earth alkaline (Ce, La, Pr etc.), alkaline earth metals (Ca, Cs, Sr, Ba etc.) and the B sites are usually occupied by transition metals (Fe, Co, Cu, Mn, Ni, and Cr). Perovskite shows high activity for CO oxidation and high thermal resistance [1]. The performance of perovskite catalysts in CO oxidation processes can be increased by fractional replacement of metal in position A and/or position B with metal cations varying in their valence number [2]. The catalytic activity of perovskite catalysts can be enhanced by the incomplete substitution of metal in position A or B with cations of noble metals like Ag, Au, Pt and Pd etc [3]. When deposited of noble metals into perovskite is main factor in the catalyst's activity, which, however, is also highly effected by the type of perovskite was used. The activity of perovskite catalyst is strongly influenced by their preparation methods [4]. The main benefit of perovskite catalysts lies in the fact that they are posses' higher activity and thermal stability compared to pure oxides [5]. The addition of noble metals into perovskite reduces sintering and reduction in mass as a consequence of volatilization at a high temperature in oxidizing conditions [6].

Increasing the number of vehicles on roads, CO concentration has reached an alarming level in urban areas. In the CO oxidation process, the oxygen is first adsorbed on the perovskite catalyst surface with the energy of activation [7]. By substituting the A and B cations, one can control the total amount of substitution and apply for suitable cations that will get important structural changes, such as lattice distortions, stabilization of multiple oxidation states or generation of cationic and anionic vacancies, all have a direct effect vary in catalytic activity [8,9]. The dispersion of perovskites on a support, one can select the most excellent matrix to contain the oxide particles and expose the major amount of

* Corresponding author.
E-mail addresses: subhasdey633@gmail.com, shubhashish.rs.civ13@itbhu.ac.in (S. Dey).

https://doi.org/10.1016/j.soh.2022.100002
Received 26 June 2022; Accepted 20 September 2022
Available online 24 September 2022

active sites in order to get the better catalytic activity for CO oxidation [10]. Perovskite-type (ABO_3) catalysts can be well modified by the partial substitution of atoms at A and/or B-sites, producing iso-structural, which may stabilize unusual oxidation states of B component, induce structural distortions and create cationic or anionic vacancies [11,12]. The best catalyst for CO oxidation could able to maintain the oxide structure throughout the process. The fast changes in temperature of wash coat and active layer on the support may break due to their thermal extension [13, 14]. Partial substitution of lanthanum perovskite increases with increases of noble metals into the catalyst. It also influenced by the time and temperature of perovskite calcination and increase with the rise in calcination temperature [15]. The size of perovskites has a smaller influence on the activity of catalysts. This catalyst exhibits good adhesion to the monolithic metal support. In geometric factors, the perovskites shows that lanthanum, which is major lanthanide ion in the series, leads to the most steady perovskite structure [16]. The substituting cations increase the activity and stability of perovskite oxide structure. Manganite and cobaltate perovskite catalysts have been reported to be highly active for CO oxidations [17,18]. In comparison to manganese-based perovskite, the cobalt-based oxides are difficult to support directly on alumina because cobalt ions easily diffuse into the bulk of support to form cobalt aluminum perovskite structure [19]. The catalytic activity of various perovskite catalysts having different compositions in CO oxidation reactions involving at various temperatures has been discussed in this review paper.

2. Structural analysis of perovskite catalysts

Perovskite-catalyst (ABO_3) can crystallize in cubic structure in space group Pmm or indistinct rhombohedral, tetragonal, orthorhombic and triclinic symmetry as represent in Fig. 1. The presence of oxygen and vacancy can be change depending on the composition due to a great stability range of structure [20]. The larger A-site cation is frequently rare earth, alkaline earth or an alkali metal cation coordinated to 12 oxygen anions. The B-site cation is usually a minor transition metal cation covering octahedral interstices in oxygen structure. Several combinations of A and B site cations can form a stable perovskite-like structure. These cations with oxygen anions can be partially substituted by other suitable elements. Electronic structure descriptions in Fig. 2 are sum of active quantities used to generate qualitative correlations for a wide range of properties. In particular, the oxygen p-band center has been used to direct material finding and basic considerate of a range of perovskite compounds for utilize in catalyzing the oxygen reduction and advancement reactions [21,22].

Partial chemical substitutions of A and/or B sites for ABO_3 type perovskite and structures drive structural and electronic transformations, foremost to functional properties such as large magneto-resistance and high-temperature superconductivity [23]. A couple of various metal ions covering equal crystallographic sites create spatial ordering of atoms, crystallizing in ordered perovskite structures with chemical formulae such as $A_2BB'O_6$, $AA'B_2O_6$ and $AA'_3B_4O_{12}$ [24]. Combinations of A, A′ and B site ions provide surprising properties, some of which are functional. The charge-disproportionate or transfer transitions are abruptly switched by bond strains on rare-earth metals. Crystal structure analysis shown in Fig. 2 suggests that metal oxygen bonds make neighboring adsorbates close enough to interact, probably facilitate two active site reaction mechanisms [25]. The conventional single-active-site reactions for plain perovskite catalysts and expected to keep away from rate-determining steps of usual mechanisms. Perovskites may be arranged in layers, with the ABO_3 structure separated by thin sheets of interfere material [26]. The various forms of intrusions, based on the chemical structure of groups are defined as:

- **Aurivillius phase**: The major layer is contained a $[Bi_2O_2]^{2+}$ ion, covering every $n$$ABO_3$ layers, foremost to an generally chemical formula of $[Bi_2O_2]$-$A_{(n-1)}B_2O_7$.
- **Dion—Jacobson phase:** The main layer is collected of an alkali metal (M) each $n$$ABO_3$ layers, giving the in general formula as $M^+A_{(n-1)}B_nO_{(3n+1)}$.
- **Ruddlesden-Popper phase**: The major layer occurs between everyone ($n = 1$) or two ($n = 2$) layers of the ABO_3 lattice.

In the cubic unit cell, the 'A' atom sits at cube corner positions (0 0 0), type 'B' atom sits at body-center position (½ ½ ½) and oxygen atoms meet at face-centered positions (½ ½ 0). The comparative ion size for steadiness of cubic structure are moderately rigid, so small buckling and warp can generate many lower-symmetry indistinguishable versions, in which the coordination numbers of A cations and B cations [27,28]. The most active oxygen reaction catalysis for quadruple perovskite oxides containing of earth-abundant elements exposed that exploitation of ultra-high-pressure preparations facilitates the increasing of novel functional materials. A large amount of perovskites compounds prepared in high pressure also shows best candidates for functional materials. Several crystal structures are closely related to perovskite structure is called hexagonal perovskites. The perovskite structure (shown in Fig. 3) contains two A-site cations with robustly various sizes are used, further complication increases from ordering of A-sites and oxygen vacancies as in the double perovskite ($AA'B_2O_{5+\delta}$) [29]. The natural of cation in ABX_3 act as a major role in the formation of structure of perovskites structure moreover a large outcome on stability and electronic property of the materials. The sharing of various cation and anions in different perovskite catalysts is shown in the Fig. 3.

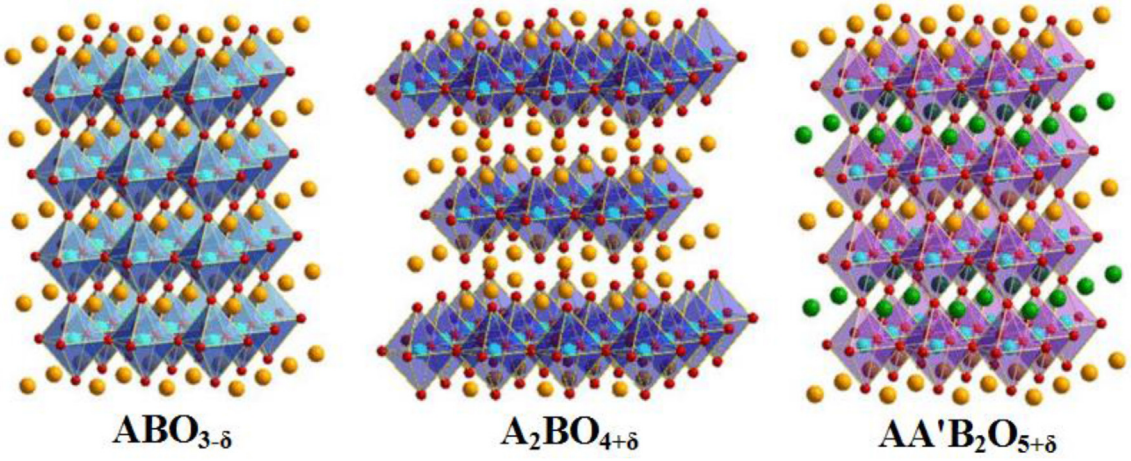

Fig. 1. Crystalline structure of various perovskite catalysts [24–26].

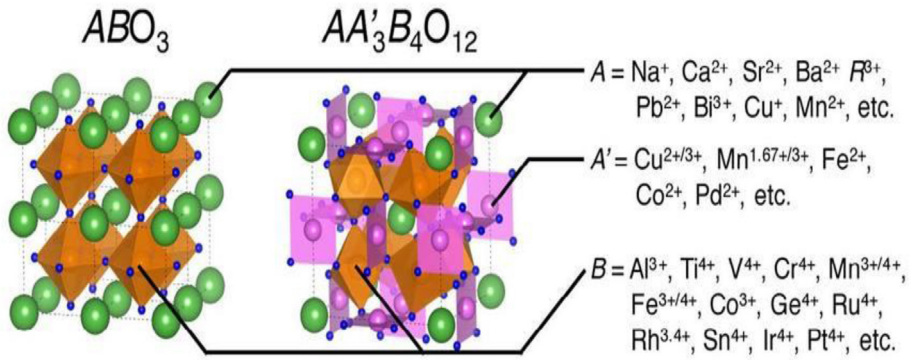

Fig. 2. Crystal structure of (ABO_3) and quadruple ($AA'_3B_4O_{12}$) perovskites [34,43,44].

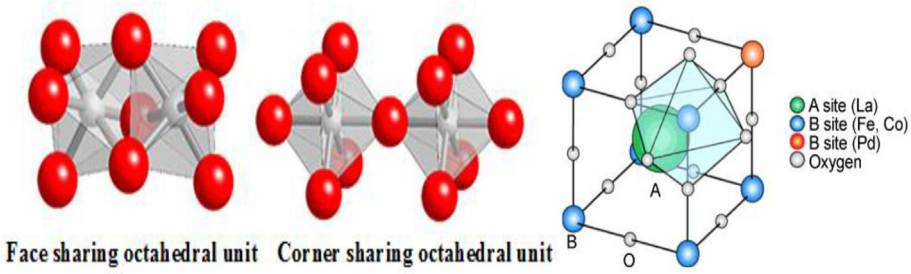

Fig. 3. Sharing group of various perovskite catalysts [11,12,18].

A cation exchange should be based on BX_6 octahedral allocation with respect to a Goldschmidt tolerance factor. A cation substitution is intentional to get more-stable and suitable dynamic position of transmission band of perovskite film. The octahedral deformation increases by increase in an ionic radius of organic cation [30]. The traditional position of perovskite lattice is discussed in Table 1. It consists of small B cations within oxygen octahedral and larger A cations which are XII fold coordinated by oxygen. The $A^{3+}B^{3+}O_3$ perovskites are most symmetric structure observed in rhombohedra structure. It involves a rotation of BO_6 octahedral with respect to cubic structure [31]. The A cations are present in corners of cube and B cation in center with oxygen ions in the face-centered positions. The decrease of A cation size will be reach where the cations will be very small to stay behind in make contact with anions in the cubic structure. The lowest lattice energy was recognized for all compounds so that an energy value was assigned to all the composition.

Table 1
Atomistic positions in various types of perovskite structure.

Structure	Site	Location
Cubic	A cation	2a
	B cation	2a
	O anion	6b
Orthorhombic	A cation	4c
	B cation	4b
	O(1) anion	4c
	O(2) anion	8d
Rhombohedral	A cation	6a
	B cation	6b
	O anion	18e
Hexagonal	A cation	2a
	A cation	4b
	B cation	6c
	O(1) anion	6c
	O(2) anion	6c
	O(3) anion	2a
	O(4) anion	4b
Cubic bixbyite	A/B cation	8b
	A/B cation	24d
	O anion	48e

The A cation is huge and B cation is lower as a result of the lowest energy structure is rhombohedral in nature. As the A cation radius decreases and B cation radius increases, the lower energy structure changes to be orthorhombic. The reducing of A cation radius and raising in B cation radius result in the creation of hexagonal structure. The lattice or internal energy does not change significantly with the changes in crystallographic structure [32]. The structures of perovskites compounds have been studied by many workers. The actual perovskite compounds with few binary oxides have simple cubic in structure as shown in Fig. 4 at room temperature and this structure maintained at higher temperatures. The X-ray patterns of many compounds can be indexed on the basis of distortion of perovskite structure [33]. In addition to various types of disturbances that involve a multiplication of pseudo cubic cell resultant in tetragonal, orthorhombic and rhombohedral symmetries. The most interests study of ferroelectric forms of perovskite structure, especially in two groups of mixed oxides $A^{+2}B^{+4}O_3$ and $A^{+3}B^{+3}O_3$. A classification of perovskite-type structures was done on the basis of radii of their metallic ions [34].

Perovskites showed excellent catalytic activity and high chemical stability; therefore, they were studied in a wide range in the catalysis of different reactions. Perovskites can be described as a model of active sites and as an oxidation or oxygen-activated catalyst. The stability of the perovskite structure allowed the compounds preparation from elements with unusual valence states or a high extent of oxygen deficiency. In Fig. 5 shows a unit cell of perovskite structure. Perovskites exhibited high catalytic activity, which is partially associated with the high surface activity to oxygen reduction ratio or oxygen activation that resulted from the large number of oxygen vacancies. Perovskites can act as automobile exhaust gas catalyst, intelligent automobile catalyst and cleaning catalyst, etc., for various catalytic environmental reactions. It was reported in the literature that perovskites containing Cu, Co, Mn, or Fe showed excellent catalytic activity toward the direct decomposition of NO at high temperature, which is considered one of the difficult reactions in the catalysis ($2NO \rightarrow N_2+O_2$). Perovskites showed superior activity for this reaction at high temperatures because of the presence of oxygen

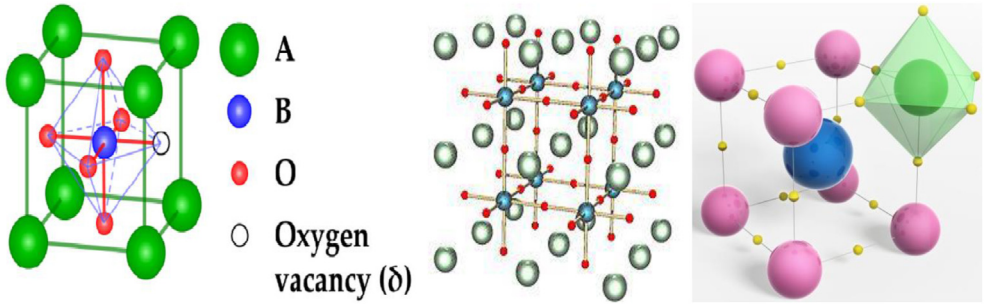

Fig. 4. Oxygen vacancy presents in the perovskite catalysts [8–10,21,22].

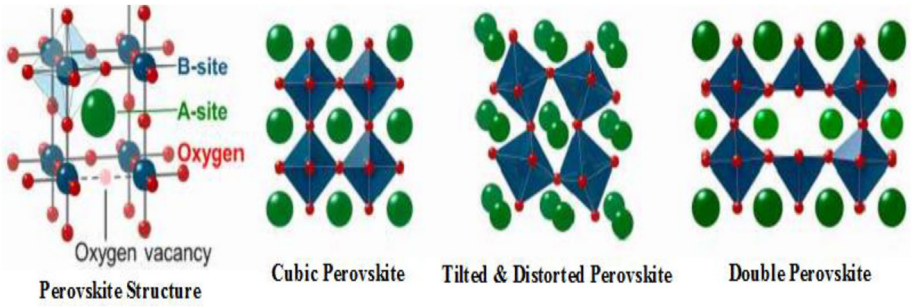

Fig. 5. Representation of a unit cell of perovskite structure [32–34,40].

deficiency and the simple elimination of the surface oxygen in the form of a reaction product. NO decomposition activity was enhanced upon doping. Also, under an atmosphere that is rich with oxygen up to 5%, Ba(La)Mn(Mg)O_3 perovskite exhibited superior activity toward the decomposition of NO.

Perovskite showed a great impact as an automobile catalyst; intelligent catalyst. Pd–Rh–Pt catalysts was utilized as an effective catalyst for the removal of NO, CO and uncombusted hydrocarbons. There is another catalyst that consists of fine particles, with high surface-to-volume ratio, and can be utilized to reduce the amount of precious metals used. However, these fine particles exhibited very bad stability under the operation conditions leading to catalyst deactivation. Therefore, the perovskite oxides can be used showing redox properties to preserve a great dispersion state. The crystalline structure of various perovskite catalysts and their formation is shown in the Fig. 6. Upon oxidation, Pd is oxidized in the form of $LaFe_{0.57}Co_{0.38}Pd_{0.05}O_3$ and upon reduction; fine metallic particles of Pd were produced with radius of 1–3 nm. This cycle resulted in partial replacement of Pd into and sedimentation from the framework of the perovskite under oxidizing and reducing conditions, respectively, displaying a great dispersion state of Pd. Also, this cycle improved the excellent long-term stability of Pd during the pollutants removal from the exhaust gas. Exposing the catalyst to oxidizing and reducing atmosphere resulted in the recovery of the high dispersion state of Pd. This catalyst is known as intelligent catalyst because of the great dispersion state of Pd and the excellent stability of the perovskite structure.

One of the important characteristic of perovskites is ferroelectric behavior, which is obvious in $BaTiO_3$, $PdZrO_3$, and their doped compounds. The ferroelectric behavior of $BaTiO_3$ was strongly related to its crystal structure. $BaTiO_3$ was subjected to three phase transitions; as the temperature increases, it was converted from monoclinic to tetragonal then to cubic. One of the major properties of perovskites is superconductivity. The halide perovskite catalyst crystalline structure is shows in the Fig. 7. Cu-based perovskites act as high-temperature superconductors, and La–Ba–Cu–O perovskite was first reported. The presence of Cu in B-site is essential for the superconductivity and various superconducting oxides can be manufactured with different A-site ions. Furthermore, some perovskites exhibited great electronic conductivity similar to that of metals like Cu. $LaCoO_3$ and $LaMnO_3$ are examples of perovskites exhibiting high electronic conductivity, and therefore they are utilized as cathodes in solid oxide fuel cells displaying superior hole conductivity of 100 S/cm. The electronic conductivity of the perovskites

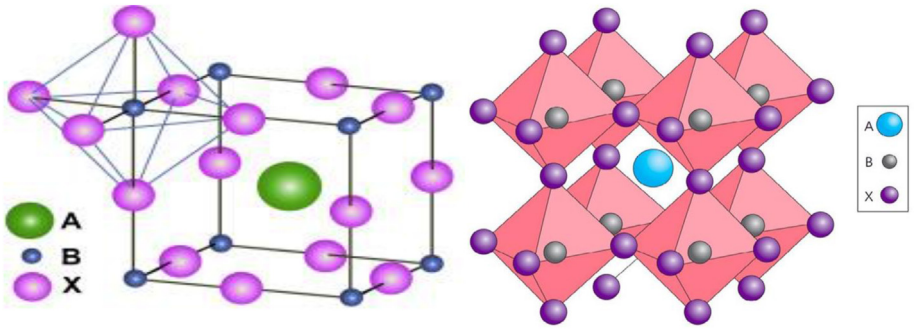

Fig. 6. Crystal structure of various perovskite catalysts [48–50].

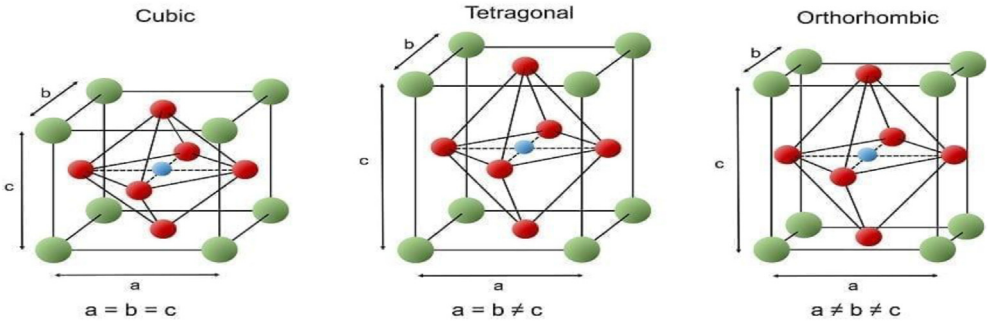

Fig. 7. Halide perovskite crystalline structure [39,40].

can be improved by doping the A-site with another cation, which resulted in increasing the amount of the mobile charge carriers created by the reparations of charges.

In the ABO_3 form, B is a transition metal ion with small radius, larger A ion is an alkali earth metals or lanthanides with larger radius, and O is the oxygen ion with the ratio of 1:1:3. In the cubic unit cell of ABO_3 perovskite, atom A is located at the body center, atom B is located at the cube corner position, and oxygen atoms are located at face-centered positions. The 6-fold coordination of B cation (octahedron) and the 12-fold coordination of the A cation resulted in the stabilization of the perovskite structure. The perfect perovskite structure was a corner linked BO_6 octahedra with interstitial A cations. Some distortions may exist in the ideal cubic form of perovskite resulted in orthorhombic, rhombohedral, hexagonal and tetragonal forms. In general, all the perovskite distortions maintaining the A and B site oxygen coordination was achieved by the tilting of the BO_6 octahedra and an associated displacement of the A cation. The different perovskite catalyst unit cell structure is shown in the Fig. 8.

Goldschmidt presented much of the early work on the synthetic perovskites and developed the principle of the tolerance factor t, which is applicable to the empirical ionic radii at room temperature. Goldschmidt presented much of the early work on the synthetic perovskites and developed the principle of the tolerance factor t, which is applicable to the empirical ionic radii at room temperature. Where r_A is the radius of the A-site cation, r_B is the radius of the B-site cation, and r_O is the radius of oxygen ion O^{2-}. The tolerance factor can be used to estimate the suitability of the combination of cations for the perovskite structure. It is a real measure of the degree of distortion of perovskite from the ideal cubic structure so that the value of t tends to unity as the structure approaches the cubic form. From the equation, the tolerance factor will decrease when r_A decreases and/or r_B increases. Based on the analysis of tolerance factor value, Hines et al. solely suggested that the perovskite structure can be estimated. For $1.00 < t < 1.13$, $0.9 < t < 1.0$, and $0.75 < t < 0.9$, the perovskite structure is hexagonal, cubic and orthorhombic, respectively. For $t < 0.75$, the structure was adopted to hexagonal ilmenite structure ($FeTiO_3$).

$$t = \frac{(r_A + r_o)}{[\sqrt{2}(r_B + r_o)]}\ BB_1$$

Electro neutrality; the perovskite formula must have neutral balanced charge therefore the product of the addition of the charges of A and B ions should be equivalent to the whole charge of the oxygen ions. An appropriate charge distribution should be attained in the forms of $A^{1+}B^{5+}O_3$, $A^{4+}B^{2+}O_3$ or $A^{3+}B^{3+}O_3$. Ionic radii requirements; $r_A > 0.090$ nm and $r_B > 0.051$ nm, and the tolerance factor must have values within the range $0.8 < t < 1.0$. Perovskite exhibited a variety of fascinating properties like ferro electricity as in case of $BaTiO_3$ and super conductivity as in case of $Ba_2YCu_3O_7$. They exhibited good electrical conductivity close to metals, ionic conductivity and mixed ionic and electronic conductivity. In addition, several perovskites exhibited high catalytic activity toward various reactions. There are some properties inherent to dielectric materials like ferroelectricity, piezoelectricity, electrostriction and pyroelectricity.

3. Methods of perovskite catalysts synthesis

3.1. Solid-state reactions

In solid-state reactions, the raw materials and the final products are in the solid-state therefore nitrates, carbonates, oxides and others can be mixed with the stoichiometric ratios. Perovskites can be synthesized via solid-state reactions by mixing carbonates or oxides of the A- and B-site metal ions corresponding to the perovskite formula ABO_3 in the required proportion to obtain the final product with the desired composition. They are ball milling effectively in an appropriate milling media of acetone or isopropanol. Then the obtained product is dried at 100 °C and calcined in air at 600 °C for 4–8 h under heating/cooling rates of 2 °C/min. After that, the calcined samples are grinded well and sieved. Then it was

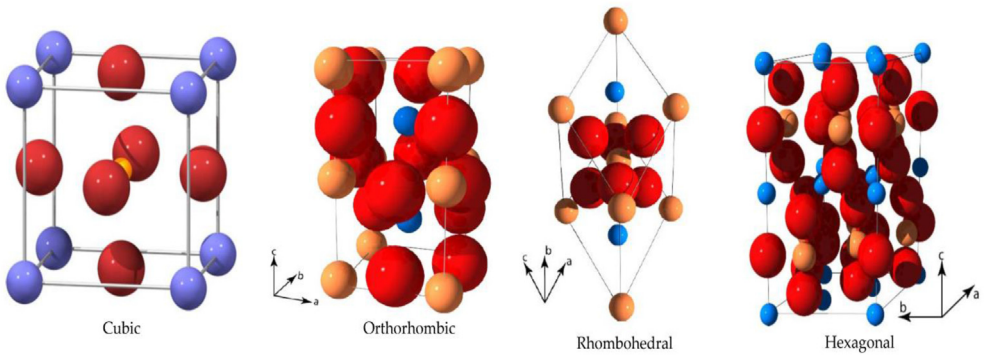

Fig. 8. Different perovskite unit cells structures [45–48,52–54].

calcined again at 1300–1600 °C for 5–15 h under the heating/cooling rate of 2 °C/min to confirm the formation of single phase of perovskite. Again grinding and sieving was carried out for the calcined samples. The synthesis of $BaCeO_3$-based proton conductor perovskites and $BaCe_{0.95}Yb_{0.05}O_{3-\delta}$ was achieved through the previous methodology using $BaCO_3$, CeO_2 and Yb_2O_3 as the starting materials and isopropanol as the milling media.

3.2. Wet chemical methods (solution preparation)

These methods included the sol-gel preparation, co-precipitation of metal ions using precipitating agents like cyanide, oxalate, carbonate, citrate, hydroxide ions, etc., and thermal treatment, which resulted in a single-phase material with large surface area and high homogeneity. These methods presented good advantages such as lower temperature compared to the solid-state reactions, better homogeneity, greater flexibility in forming thin films, improved reactivity and new compositions and better control of stoichiometry, particle size, and purity. Therefore, they opened new directions for molecular architecture in the synthesis of perovskites. Solution methods were classified based on the means used for solvent removal. Two classes were identified: (i) precipitation followed by filtration, centrifugation, etc., for the separation of the solid and liquid phases and (ii) thermal treatment such as evaporation, sublimation, combustion, etc., for solvent removal. There are several factors must be taken in consideration in solution methods like solubility, solvent compatibility, cost, purity, toxicity, and choice of presumably inert anions.

3.3. Precipitation

3.3.1. Oxalate-based preparation

This method is built on the assimilation of oxalic acid with carbonates, hydroxides, or oxides producing metal oxalates, water and carbon dioxide as products. The solubility problem is minimized as the pH of the resulting solution is close to 7. An oxidizing atmosphere like oxygen was used during calcination to avoid the formation of carbide and carbon residues. It utilized an aqueous chloride solution with oxalic acid to obtain unique and novel complex compound of $BaTiO(C_2O_4)_2.4H_2O$ as a precursor for the preparation of finely divided and stoichiometric $BaTiO_3$.

3.3.2. Hydroxide-based preparation

This method is often used due to its low solubility and the possible variety of precipitation schemes. The sol-gel process can be used to produce a wide range of new materials and improve their properties. It presented some advantages over the other traditional methods like chemical homogeneity, low calcination temperature, room temperature deposition, and controlled hydrolysis for thin film formation. $BaZrO_3$ powders in its pure crystalline form can be prepared by the precipitation in aqueous solution of high basicity. $LaCoO_3$ was prepared by the simultaneous oxidation and coprecipitation of a mixture containing equimolar amounts of La(III) and Co(II) nitrates producing a gel containing hydroxide then calcination at 600 °C.

3.3.3. Acetate-based preparation

Different perovskites were prepared by mixing acetate ions alone or together with nitrate ions with the metal ions salts. $La_{1-x}Sr_xCoO_3$ with $x = 0, 0.2, 0.4, 0.6$ was prepared using acetate precursors then calcination at 1123 K in air for 5 h $La_{1-x}Sr_xCo_{1-y}Fe_yO_3$ was prepared using iron nitrate and strontium, cobalt and lanthanum acetates then calcination at 1123 K in air between 5 and 10 h.

3.3.4. Citrate-based preparation

Citrate precursors can be used and undergo several decomposition steps in the synthesis of perovskite. These steps included the decomposition of citrate complexes and removal of CO_3^{2-} and NO_3 ions. $LaCo_{0.4}Fe_{0.6}O_3$ can be prepared by this method, and the mechanism was investigated by thermo-gravimetry, XRD, and IR spectroscopy.

3.4. Thermal treatment

3.4.1. Freeze-drying

The freeze-drying method can be achieved through the following steps: (i) dissolution of the starting salts in the suitable solvent, water in most cases; (ii) freezing the solution very fast to keep its chemical homogeneity; (iii) freeze-drying the frozen solution to get the dehydrated salts without passing through the liquid phase; and (iv) decomposition of the dehydrated salts to give the desired perovskite powder. The rate of heat loss from the solution is the most important characteristic for the freezing step. This rate should be as high as possible to decrease the segregation of ice-salt. Also, in case of multi-component solutions, the heat loss rate should be high to prevent the large-scale segregation of the cation components.

3.4.2. Plasma spray-drying

This method was applicable to various precursors, including gaseous, liquid, and solid materials. It was applied for the preparation of various ceramic, electronic, and catalytic materials. It presented many advantages in terms of economy, purity, particle size distribution, and reactivity. This method was achieved through two steps: (i) injection of the reactants and (ii) generation and interaction of the molten droplets (with substrate or with the previously generated droplets). The thick film of $YBa_2Cu_3O_x$ covering large areas was prepared via this approach, and the optimum superconducting oxide phase was obtained by varying the preparation conditions like plasma parameters, substrate temperatures, and film post deposition treatment.

3.5. Combustion

A redox reaction, which is thermally induced, occurs between the oxidant and fuel. A homogenous, highly reactive, and nanosized powder was prepared by this method. When compared with the other traditional methods, a single-phase perovskite powder can be obtained at lower calcination temperatures or shorter reaction times. One of the most popular solution combustion methods is citrate/nitrate combustion, where citric acid is the fuel and metal nitrates are used as the source of metal and oxidant. It is similar to the Pechini process “sol-gel combustion method” to a large extent, but in citrate/nitrate combustion, ethylene glycol or other polyhydroxy alcohols are not used. In addition, in citrate/nitrate combustion, the nitrates are not eliminated in the form of NOx, but they remain in the mixture with the metal-citrate complex facilitating the auto-combustion. Iron, cobalt, and cerium-perovskite can be prepared via citrate/nitrate combustion synthesis. In addition, uniform nanopowder of $La_{0.6}Sr_{0.4}CoO_{3-\delta}$ was prepared by the combined citrate–EDTA method, where the precursor solution was made of metal nitrates, citric acid and EDTA under controlled pH with ammonia. $La_{0.8}Sr_{0.2}Co_{0.2}Fe_{0.8}O_{3-\delta}$ and Sr or Ce-doped $La_{1-x}M_xCrO_3$ catalysts were prepared by citrate/nitrate combustion method. Furthermore, the Pechini “citrate gel” process includes two stages: (i) a complex was formed between the metal ions and citric acid, then (ii) the produced complex was polyesterified with ethylene glycol to maintain the metal salt solution in a gel at a homogenous state. This approach presented some advantages like high purity, minimized segregation and good monitoring of the resulting perovskite composition. $LaMnO_3$, $LaCoO_3$, and $LaNiO_3$ were prepared by citric acid gel process producing nanophasic thin films.

3.6. Microwave synthesis

The microwave irradiation process (MIP), evolving from microwave sintering, was applied widely in food drying, inorganic/organic synthesis, plasma chemistry, and microwave-induced catalysis. MIP showed

fascinating advantages: (i) fast reaction rate, (ii) regular heating, and (iii) efficient and clean energy. The microwave preparations were achieved in domestic microwave oven at frequency of 2.45 GHz with 1 kW as the maximum output power. Dielectric materials absorbed microwave energy converted directly into heat energy through the polarization and dielectric loss in the interior of materials. The energy efficiency reached 80–90% which is much higher than the conventional routes. MIP was recently utilized to prepare perovskites nanomaterials reducing both the high temperature of calcination (higher than 700 °C) and long time (greater than 3 h) required for pretreatment or sintering. $GaAlO_3$ and $LaCrO_3$ perovskites with ferroelectric, superconductive, high-temperature ionic conductive and magnetic ordering properties, faster lattice diffusion, and grain size with smaller size were prepared in MIP. The $CaTiO_3$ powders prepared in MIP presented a fast structural ordering than powders dealt in ordinary furnace. Hydrothermal conventional and dielectric heating were utilized to prepare La–Ce–Mn–O catalysts. Hydrothermal MIP leads to formation of $La_{1-x}Ce_xMnO_{3+\varepsilon}CeO_2$ ($x + \varepsilon = 0.2$) with enhanced catalytic activity while using the conventional heating methods lead to formation of $LaMnO_3 + CeO_2$. Moreover, nanosized single-phase perovskite-type $LaFeO_3$, $SmFeO_3$, $NdFeO_3$, $GdFeO_3$, barium iron niobate powders, $KNbO_3$, $PbWO_4$, $CaMoO_4$ and MWO_4 (M: Ca, Ni), strontium hexaferrite and $SrRuO_3$ were prepared in MIP showing finer particles, higher specific surface areas and shorter time for synthesis of single crystalline powders.

4. Chemisorptions of carbon monoxide over perovskite catalysts

Perovskites showed a good catalytic activity, which is moderately associated with more surface activity to oxygen decline ratio or oxygen activation that creates from huge amount of oxygen vacancies. It can act like a catalytic converter and cleaning catalyst, etc., for different catalytic environmental reactions [35]. Perovskites containing Cu, Co, Mn or Fe showed excellent catalytic activity toward direct oxidation of CO at high temperature. The $LaCoO_3$, $LaMnO_3$ and $BaCuO_3$ perovskite catalysts showed great catalytic activity for CO oxidation at higher temperatures. The perovskites represents best activity for reaction at high temperatures because the presence of oxygen shortage and easy removal of surface oxygen in the form of reaction product. The addition of smaller amounts of element in perovskite catalyst improved their performances. The $Cu_{0.15}Ce(La)_{0.85}Ox$ catalyst synthesized by wet impregnation method showed that the best activity toward CO oxidation [36]. It fine particles with high surface-to-volume ratio be capable of utilized to decrease the amount of noble metals used. However, the fine particles bad stability in operation conditions mostly to catalyst deactivation. So that it can be used to the showing redox properties to maintain a more dispersion state [37]. Lanthanum (La) is oxidized in the form of various La oxide catalysts with fine metallic particles of La were produced in a radius of 1–3 nm. The $LnCoO_3$ catalyst is known as an intelligent catalyst because of great dispersion state of Ln and excellent stability of perovskite structure. The different properties of perovskites and their catalytic activity are highly affected by the method of preparation, calcinations conditions and A- and/or B-site substitutions [38,39].

The doping in perovskite catalysts the catalytic activity, ionic radius, electronic conductivity, physical and chemical properties can be changed for exploitation in different applications. Different cations with various sizes and charges can be hosted in perovskites; thus, many studies can be performed to utilize doped perovskites in CO oxidation [40,41]. The chemisorptions of CO and CH_4 over perovskite catalysts are shown in the Fig. 9. The material characteristics of perovskite oxides mainly related with structural characters were very much affected by structural changes from perfect cubic structure of perovskite catalysts. The synergism effect between the crystal lattice of perovskite and metal ions dissolved in lattice upon doping [42]. It results in an improved redox reaction and best catalytic activity of synthesized perovskite was obtained. A remarkable modifies in transportation and magnetic properties of ABO_3 perovskite can be done by doping in the B-site due to an ionic valence effect and/or anionic size effect. The doping in B-site of ABO_3 perovskites with transition metals mainly noble metals, the strength of perovskite was enhanced and catalytic activity was improved considerably [43]. In $LaMnO_3 + CeO_2$ perovskites with a low surface area (<15 m^2/g) the Ce^{4+} replacement into La^{3+} sites reduces both cell parameters of rhombohedral unit cell and crystalline domain sizes, since the ionic radius of Ce^{4+} is lesser than La^{3+}. The selective of CO oxidation in which CO and O_2 were totally converted into CO_2 and presence of cerium affected the reaction kinetics shifting CO conversion to higher temperatures [44]. The Ce^{4+} distorted some Co^{3+} to Co^{2+} to maintain the charge neutrality within the $LaxCe_{1-x}CoO_3$ structure, as a result decreasing the amount of active Co^{3+} sites on the $LaCoO_3$ surface and declining the activity for CO oxidation. The charge neutrality would stabilize the total Co^{3+}/O_2 on the surface, ensuring high CO_2 selectivity for cerium substituted perovskites [45]. The effect of strontium insertion into $La_{0.5}Sr_{0.5}CoO_{3-d}$ on the catalytic performance of CO oxidation was discussed in Table 2 (see Fig. 10).

Differently, from Ceria the Sr^{2+} as a cationic dopant is probable to raise cobalt oxidation state and/or produce oxygen vacancies inside the crystal lattice, it was the oxygen mobility and supply lattice oxygen for CO oxidation on the surface [46]. The complete Sr^{2+} substitution into the rhombohedral crystalline structure of perovskite which led to declined and extension of unit cell volume, since the ionic radius of Sr^{2+} (0.132 nm) is superior than La^{3+} ion. In $LaFeO_3$ molecular oxygen chemisorbs on Fe^+ cations as an O^{2-} anion, dissociating to form atomic oxygen (O^-) on the iron sites. The CO adsorbs on the surface oxide ions formed a labile species that interacts with adsorbed atomic oxygen, producing carbonates which decompose towards CO_2 and oxygen [47]. The manganese promoted $La_{0.7}Sr_{0.3}Mn_{1-X}Co_XO_3$ perovskites were investigated as a catalyst in the CO oxidation reactions. Increasing the amount of Mn atoms on the $La_{0.7}Sr_{0.3}Mn_{1-X}Co_XO_3$ catalyst surfaces affecting the catalytic behavior: the greater $Co^o + Mn^0$ exposition. The higher extension of $La_{0.7}Sr_{0.3}Mn_{1-X}Co_XO_3$ phase derived from the

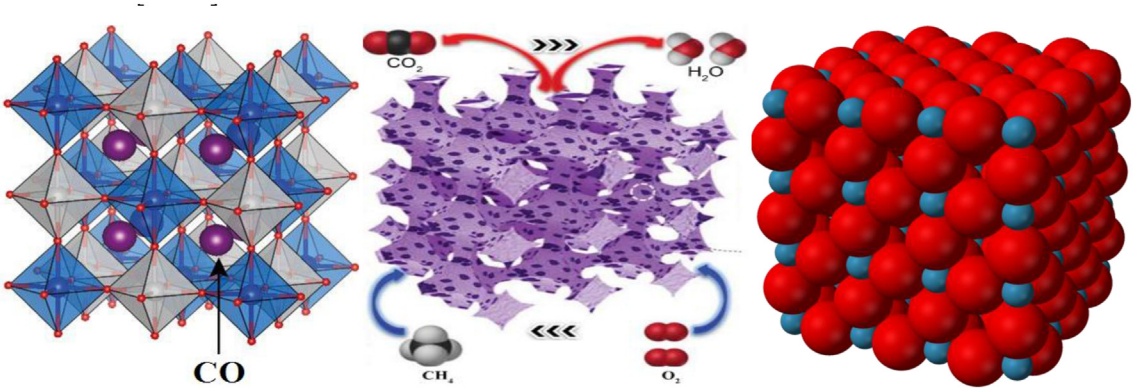

Fig. 9. Chemisorptions of CO over various perovskite catalysts [56–58,62–64].

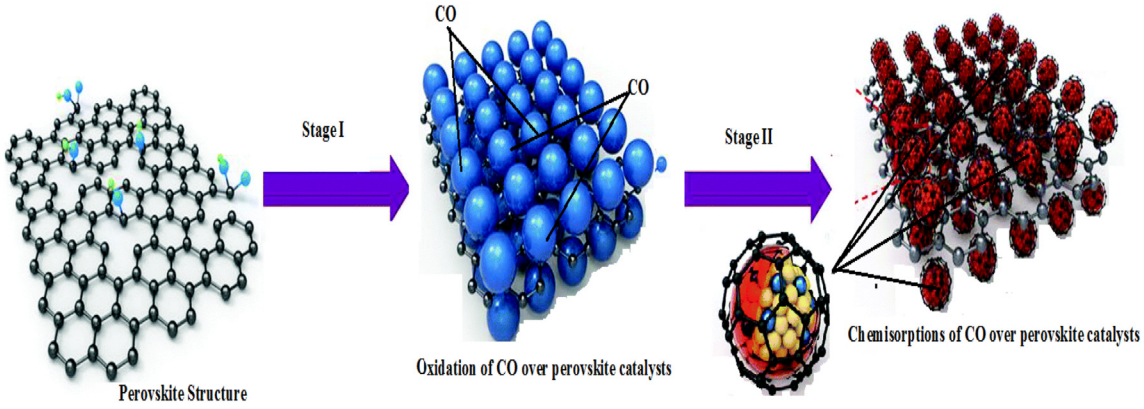

Fig. 10. Carbon monoxide oxidation over perovskite catalysts [60–62].

perovskite structure, higher the activity and stability of the catalysts. In $Zn_{1-X}Ni_XMnO_3$ catalyst the complete conversion of CO was obtained at 300 °C [48].

This catalyst is highest resistance to carbon deposition among all the catalysts. The rhombohedral structure of perovskite towards metallic Ni^0 and hexagonal Mn_2O_3 phases (for high Zn content, ZnO and Ni_XMnO_3 phases also emerged). The fractional replacement of Ba by Zn in $La_{0.9}Ba_{0.1}CoO_3$ raising the oxidation temperature of perovskite, signifying a more constant structure in reaction conditions which might be stay away from Ba sintering [49]. In $LaMn_{1-x}Cu_xO_{3+\S}$ perovskites the Cu replacement could enhance the amount of chemisorbed oxygen species over the perovskite, improving the catalytic activity for CO oxidation. The addition of iron (Fe) in $LaFe_{0.8}Co_{0.2}O_3$ lattice the iron valence changed from Fe^{3+} to Fe^{4+} improving the catalytic performance [50]. The A series of B site replacements over $LaCoO_3$ perovskite showed that Mn^{2+}, Fe^{2+}, Ni^{2+} and Cu^{2+} dopants could get better CO conversion. To modify the characteristics of supported metal catalysts obtained from precursor perovskite under oxidation conditions. The important catalytic reactions made to better comprehend the role of active sites on the perovskite-type oxides [51].

4.1. Mechanism of CO oxidation on the perovskite catalysts

The efficiency of perovskite catalysts for reactions with CO molecules is strongly depending upon the chemisorptions process. The discrete reaction mechanisms are steady with the observed kinetics [51,52]. A better device for measuring the activity of perovskite catalysts for CO oxidation is reported the activation energy of the process. Early study represented that the catalyst starting oxidized CO before its oxidized by air, and this is an investigation of a Mars-van Krevelen-type mechanism which has consequently found support [53]. The perovskite oxides frequently exhibit strong electronic and/or magnetic correlations, band gaps and bending, which may affect the mechanism. Various synthesis methods have been presented in Table 2 intended at increasing the surface area mainly mixed oxide and fast synthesis; still the surface areas between 5 and 50 m^2/g at most are achieved [54,55]. The macro-porous perovskite catalysts illustrate better catalytic activities for CO oxidation than consequent nanometric sample. Calcination temperature highly affects the crystallization and particle size of perovskite catalyst [56].

In the calcination of perovskite at higher temperature raise the crystalline and particle size. Carbon monoxide can be adsorbed either in a linear or bridged form covering respectively over perovskite catalysts. Which structure is formed depends on the chemisorptions conditions and nature of support. The CO adsorbed on perovskite could react with oxygen held by these species. This catalyst able to absorb oxygen at low temperature suggests that the CO oxidation should be done at low temperatures. The activation of surface oxygen vacancy in the perovskite catalysts performance for CO oxidation is properly represents in the Fig. 11.

However, the catalytic activity of perovskite catalyst is quite low in spite of fact that catalysts contain adsorption sites both for CO and O_2 adsorption. It causes a result of no dissociative adsorption of oxygen. The reaction mechanism of perovskite catalysts is represents in the Fig. 12. In stoichiometry of CO oxidation reaction needs the dissociation of oxygen molecules followed by reaction between adsorbed oxygen atom and CO to CO_2 is one of the accepted mechanisms for CO oxidation. In this condition, the reaction rate is limited by the dissociation of O_2. The molecular adsorption of CO occurs at higher temperatures, which ensures that the appearance of reactive oxygen forms [57,58].

The oxygen adsorption occurs mainly in the form of O_2^-, while above the calcination temperature of 350 °C the O^- species is predominate. The O^- ions are highly active and reactivity of superoxide is also high, though much lower as compared to O^-. In oxygen species, the CO molecules from gas phase can be directly oxidized [59]. The marsvan krevelen mechanism for conversion of CO over perovskite catalysts is shown in the Fig. 13. The conversion of CO by the Mars-van Krevelen mechanism would give details the relationship between easiness of catalyst activity and reducibility. Different mechanisms have been suggested for the oxidation of CO over metals and metal oxides. The CO oxidation over metals is thought to follow a Langmuir-Hinshelwood mechanism [60]. The CO_2 produced is poorly adsorbed and does not influence the rate substantially, since it's rapidly desorbed to the gas phase. The rate of reaction will be proportional to the total coverage of O_{ads} and CO_{ads} [61].

$$O_{2(g)} \rightarrow O_{2(ad)}^- \rightarrow 2O_{(ad)}^- \quad (1)$$

$$CO_{(g)} \rightarrow CO_{(ad)} \quad (2)$$

$$CO_{(ad)} + 2O_{(ad)}^- \rightarrow CO_{3(ad)}^{2-} \quad (3)$$

$$CO_{3(ad)}^{2-} \rightarrow CO_{2(ad)} + O_{(ad)}^{2-} \rightarrow CO_{2(g)} + O_{2(ad)}^- \quad (4)$$

$$O_2 + 2^* \rightarrow 2O_{ads} \quad (5)$$

$$CO + ^* \rightarrow CO_{ads} \quad (6)$$

$$CO_{ads} + O_{ads} \rightarrow CO_2 + 2^* \quad (7)$$

The procedure of CO oxidation does not take place as long as the adsorbed molecules of O_2 change to the reactive form of oxygen. The variation of activity and the binding energy of perovskite catalysts as a function of tolerance factor for the series of catalysts. The high spin state of perovskite catalysts at the surface may be favorable for the strong chemisorptions of oxygen which accounts for increased activity [62]. As far as catalyst development is concerned, it is critical to discover the structure–activity correlation of catalysts. A Langmuir-hinshelwood

Table 2
The operating parameters and activity measurement of various perovskite catalysts for CO oxidation.

Catalyst	Catalyst Preparation Method	Operating Parameters	Remarks	References
$La_{0.5}Sr_{0.5}CoO_{3-d}$	Spray pyrolysis method	The 100 gm catalyst at a flow rate of 100sccm with reactants gas mixture 1% CO and 6% O_2 in volume, a heating rate of 1 °C/min.	$La_{0.5}Sr_{0.5}CoO_{3-d}$ (T_i = 200 °C T_{50} = 300 °C, T_{100} = 500 °C)	[1]
$LnCoO_3$	Cobalt cyanide method	The 1 gm catalyst with a feed gas composition 5% CO, 5 %O_2, 90% N_2 at space velocity 19-48 h^{-1} has been used.	$LnCoO_3$ (T_i = 200 °C T_{50} = 240 °C, T_{100} = 300 °C)	[2]
Sr-doped $LaMnO_3$	Solid state diffusion process.	The 100 gm of catalyst in presence of 15.5% O_2 and 6% CO in a stream at a pressure 1.65 bar for 2 h. The temp. was carried out 500 °C and 550 °C temp.	Sr-doped $LaMnO_3$ (Xco = 60% at 520 °C)	[3]
$Cu_{0.15}Ce(La)_{.85}$ Ox	Conventional Wet impregnation method	The 100 gm catalyst with a gas mixture of 0.1% CO, 0.228% CH_4 and 1% O_2 with contact time 9 s.	$Cu_{0.15}(Ce(La))_{.85}Ox$ (T_i = 30 °C T_{50} = 70 °C, T_{100} = 95 °C)	[4]
$La_{0.8}Sr_{0.2}MnO_{3+X}$	Sol–gel method.	The 10 gm catalyst, sieved to 1.5 mm particles with feed gas composed of CO (500ppmv) in air and space velocity is 20 h^{-1}.	$La_{0.8}Sr_{0.2}MnO_{3+X}$(Xco = 100% at 400 °C)	[5]
$LaCoO_3$	Conventional pyrolysis Method	The 200 gm catalyst under a reactant stream (25 ml/min) containing 5.6mol % CO, 5.6 mol % O_2 and rest being N_2.	$LaCoO_3$ (T_i = 90 °C T_{50} = 190 °C, T_{100} = 260 °C)	[6]
$La_{1-X}Sr_XFeO_3$	Wet impregnation method	The 250 gm catalyst at temp. 250 °C for 1hr. with exposure to the reaction gas mixture at 6 kPa (CO: O_2 = 2:1).	$La_{1-X}Sr_XFeO_3$ (Xco = 70% at 720 °C)	[7]
$La_{1-X}Sr_xBO_3$	Alkaline Co-precipitation method	The 300 gm catalyst with a gaseous mixture of NO (1500 ppm), CO (1500 ppm), and He (balance) was fed into the reactor at a flow rate of 120 mL/min, and heating rate 10 °C/min.	$La_{1-X}Sr_xBO_3$ (T_i = 200 °C T_{50} = 350 °C, T_{100} = 650 °C)	[8]
$LaCoO_3$ Supported perovskite	Co-precipitation method	The 150 gm catalyst was performed at 100–550 °C temperature with a space velocity of 18950/hr. The gas mixture consists of 2% CO, 2.5% propylene and balance N_2 with feed gas.	$BaFeO_3/ZrO_2$ (T_i = 200 °C T_{50} = 320 °C, T_{100} = 400 °C) $BaFeO_3/Al_2O_3$ (T_i = 200 °C T_{50} = 420 °C, T_{100} = 500 °C) $LaFeO_3/ZrO_2$ (T_i = 200 °C T_{50} = 300 °C, T_{100} = 480 °C) $LaFeO_3/Al_2O_3$ (T_i = 200 °C T_{50} = 420 °C, T_{100} = 480 °C)	[9]
$LaSrNiO_4$	Combustion method	The 600 gm catalyst with feed gas composition 1% CO/He + 0.5–2% O_2/He; W/F = 0.6gscm^{-3}, at temperature = 300 °C.	$LaSrNiO_4$ (T_i = 250 °C T_{50} = 290 °C, T_{100} = 325 °C)	[10]
$LaCoO_3$	Reactive grinding and Citrate method	The 5 gm of catalyst with (CO: 7.8%, O_2: 13%, N_2 : 79%, SV: 32,000 Ncm^{3}g^{-1}h^{-1})	Reactive grinding (T_i = 250 °C T_{50} = 400 °C, T_{100} = 500 °C) Citrate method (T_i = 10 °C T_{50} = 500 °C	[11]
$LaMn_{1-x}Cu_xO_3$	Citrate method	A gas mixture of CO(1.3%), O_2 (1.3%) and N_2 (balance) at a flow rate 200 cm^3 min^{-1} over a 3–20 gm catalyst and GHSV = 1.8 x l0^6 h^{-1}, stream at 873 K for 1h.	$LaMn_{1-x}Cu_xO_3$ (T_i = 200 °C T_{50} = 320 °C, T_{100} = 400 °C)	[12]
$LaMn_{1-x}Cu_x$ $O_{3+§}$	Sol-gel method	The 200 gm catalyst with a total gas flow rate 50 cm^3/min. A mixture of 2% CO and 20% O_2 in nitrogen was used.	$LaMn_{1-x}Cu_x$ $O_{3+§}$ (T_i = 50 °C T_{50} = 225 °C, T_{100} = 350 °C)	[13]
$CaTiO_3$	Citrate process	The 300 gm catalyst with a gas mixture of (CO/O_2 = 2.36) at air 1.2 L/h. The reaction temp. 400 K with flow velocity of 60 mL/min.	$CaTiO_3$ (T_i = 300 °C T_{50} = 420 °C, T_{100} = 500 °C)	[14]
$LaMnO_3$ $La_{0.5}Sr_{0.5}Mn_{0.3}$	Impregnation method	The 100 gm catalyst with feed gas composition 8% CO, 4% O_2, 88% He. The total flow rate 100 sccm/min with Space velocity = 6000 h^{-1}L.	$LaMnO_3$ (T_i = −175 °C T_{50} = 275 °C, T_{100} = 460 °C) $La_{0.5}Sr_{0.5}Mn_{0.3}$ (T_i = −150 °C T_{50} = 250 °C, T_{100} = 440 °C)	[15]
$LaCoO_3$	Conventional citrate method	The 100 gm catalyst with a gas mixture of 2 vol % CO and 98 vol % air (GHSV) of 12,000 h^{-1}. The total flow rate 100 ml/min.	$LaCoO_3$ (T_i = 50 °C, T_{50} = 110 °C,T_{100} = 160 °C	[16]
$LaFeO_3$ $LaFe_{0.8}Co_{0.2}O_3$	Sol gel method	The 100 gm catalyst with feed gas composition 0.25% CO and 5% O_2 balanced He. The total gases flow rate was 50 SCCM.	$LaFeO_3$ (T_i = 200 °C, T_{50} = 266 °C, T_{100} = 320 °C) $LaFe_{0.8}Co_{0.2}O_3$ (T_i = 60 °C, T_{50} = 120 °C, T_{100} = 155 °C)	[17]
$PrMnO_3$ substitute Ba/K/Ce	Sol-gel method	The 100 gm catalyst with heating rate 50 °C/min and flow rate 60 ml/min. The gas mixture was consisting of 1% CO/1% O_2/50% H_2/N_2.	$PrMnO_3$ (T_i = 135 °C,T_{50} = 180 °C, T_{100} = 220 °C) $PrMnO_3$ substitute Ba (T_i = 65 °C,T_{50} = 110 °C, T_{100} = 160 °C) $PrMnO_3$ substitute K (T_i = 180 °C,T_{50} = 260 °C, T_{100} = 315 °C) $PrMnO_3$ substitute Ce (T_i = 105 °C,T_{50} = 145 °C, T_{100} = 220 °C)	[18]
$LaFeO_3$	Citric acid complexing method	The 100 gm catalyst with feed gas composition of 1 vol % CO, 20 vol % O_2, and He balanced. The total flow rate was 100 mL/min and space velocity was 20,000 mL/g.h.	$LaFeO_3$ (T_i = 50 °C,T_{50} = 120 °C, T_{100} = 170 °C)	[26]
$La_XK_{1-X}CoO_3$	Sol-gel method	The 100 gm catalyst with reaction gases mixture consist of 10% O_2, 0.2% CO balanced He. The total flow rate was 50 mL/min.	$LaCoO_3$ (T_i = 110 °C,T_{50} = 155 °C, T_{80} = 200 °C) $La_XK_{1-X}CoO_3$ (T_i = 145 °C,T_{50} = 210 °C, T_{80} = 260 °C)	[20]
$Zn_{1-X}Ni_XMnO_3$	Co-precipitation method	The 100 gm catalyst with feed gas composition of 5% CO and 5% O_2 in nitrogen. The flow rate was100 ml/min and GHSV was 20,000 h^{-1}.	$ZnMnO_3$ (T_i = 200 °C, T_{50} = 300 °C, T_{80} = 400 °C Const.) $Zn_{1-X}Ni_XMnO_3$ (T_i = 115 °C,T_{50} = 170 °C, T_{100} = 300 °C)	[21]
$LaCo_{0.5}M_{0.5}O_3$ (M = Mn, Cr, Fe, Ni, Cu)	Impregnation method	The 2.7 gm catalyst with feed gas flow rate was 550 cm^3/min and composition of 1.5 vol % CO and balance air was used.	$LaCoO_3$ (T_i = 150 °C, T_{50} = 210 °C, T_{100} = 450 °C) $LaCo_{0.5}Ni_{0.5}O_3$ (T_i = 145 °C,T_{50} = 175 °C,	[22]

(*continued on next page*)

Table 2 (*continued*)

Catalyst	Catalyst Preparation Method	Operating Parameters	Remarks	References
			T_{100} = 350 °C) $LaCo_{0.5}Fe_{0.5}O_3$ (T_i = 105 °C,T_{50} = 180 °C, T_{100} = 340 °C) $LaCo_{0.5}Cu_{0.5}O_3$ (T_i = 150 °C,T_{50} = 240 °C, T_{100} = 440 °C) $LaCo_{0.5}Mn_{0.5}O_3$ (T_i = 145 °C,T_{50} = 190 °C, T_{100} = 300 °C) $LaCo_{0.5}Cr_{0.5}O_3$ (T_i = 155 °C,T_{50} = 195 °C, T_{100} = 440 °C)	
$LaMnO_3 + CeO_2$	Co-precipitation method	The 50 gm catalyst in presence of 1 vol % CO, 1 vol % O_2 in 98 vol % He with a heating rate 5 K/min and space velocity was $2*10^{-2}$ $m^3s^{-1}kg^{-1}$.	$LaMnO_3 + CeO_2$ (T_i = 78 °C,T_{50} = 145 °C, T_{100} = 252 °C)	[23]
$La_{0.9}Ba_{0.1}CoO_3$	Sol-gel method	The 100 gm catalyst in presence of 500 ppm CO, 10% O_2 balanced He, with a total flow rate 50 SCCM and space velocity 30,000 h^{-1}.	$LaCoO_3$ (T_i = 170 °C,T_{50} = 240 °C, T_{100} = 300 °C) $La_{0.9}Ba_{0.1}CoO_3$ (T_i = 120 °C,T_{50} = 162 °C, T_{100} = 200 °C)	[24]
$LaBO_3$(B⎯Mn, Fe, Co)	Hydrolysis Co-precipitation method	The 100 gm catalyst in presence of 0.5% CO, 5% O_2 and He was balanced. The total flow rate was 100 ml/min and WHSV 60,000 mL/gh.	$LaMnO_3$ (T_i = 200 °C,T_{50} = 300 °C, T_{100} = 390 °C) $La_{0.8}Sr_{0.2}MnO_3$ (T_i = 150 °C,T_{50} = 250 °C, T_{100} = 340 °C) $LaCoO_3$ (T_i = 150 °C,T_{50} = 240 °C, T_{100} = 350 °C) $La_{0.8}Sr_{0.2}CoO_3$ (T_i = 100 °C,T_{50} = 160 °C, T_{100} = 240 °C) $LaFeO_3$ (T_i = 250 °C, T_{20} = 350 °C Const.) $La_{0.8}Sr_{0.2}MnO_3$ (T_i = 200 °C,T_{50} = 315 °C, T_{100} = 400 °C)	[30]
$La_{0.7}Sr_{0.3}Mn_{1-x}Co_xO_3$	Citrate method	The 200 gm catalyst in presence of 6% CO in Ar with air. The total flow rate was 47 cm^3/min and GHSV 12,000 h^{-1}.	$La_{0.7}Sr_{0.3}Mn_{1-x}Co_xO_3$ (T_i = 50 °C,T_{50} = 150 °C, T_{100} = 170 °C)	[31]
Alumina supported $LaCoO_3$	Pechini method	The 150 gm catalyst in presence of 1 vol % CO, 1 vol % O_2, 60 vol % H_2 balanced N_2 at a flow rate 100 cm^3/min.	Alumina supported $LaCoO_3$ (T_i = 100 °C,T_{50} = 170 °C, T_{100} = 300 °C)	[32]
$LaSrCuO_4$	Conventional citrate route	The 100 gm catalyst with a gas mixture of 2 vol % CO and 98 vol % air was fed into the catalyst bed at a gas hourly space velocity (GHSV) was 12,000 h^{-1}.	$LaSrCuO_4$ (T_i = 60 °C,T_{50} = 145 °C, T_{100} = 180 °C)	[33]

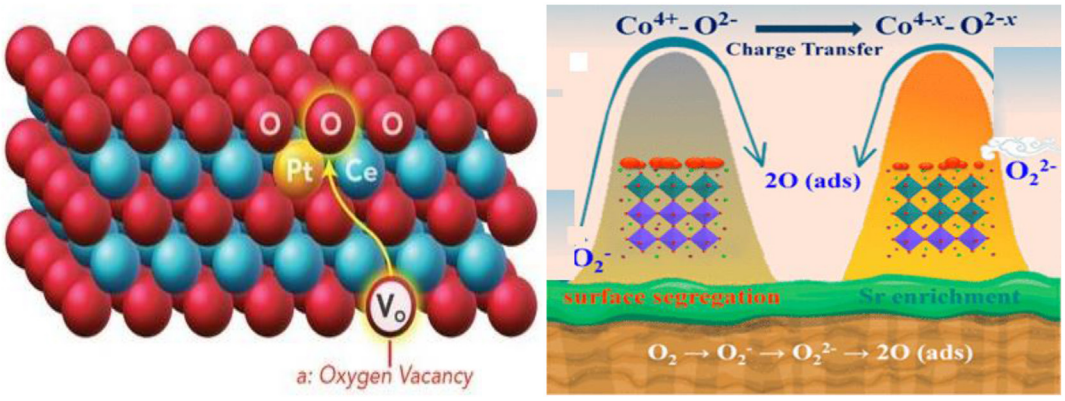

Fig. 11. Activation of surface oxygen vacancy in the perovskite catalysts [70–74].

mechanism predicts the reactivity of perovskite catalysts in CO oxidation. Low lattice oxygen mobility and kinetic effect of O_2 rule out the MvK redox mechanism [63]. Under reaction conditions, the rate was proportional to the O_2 pressure and independent of CO pressure. The rate of CO oxidation was done by following either rate of formation of CO_2 or, when the CO was intent and rate of losing of CO [64]. The mechanism for CO oxidation over perovskite catalysts shows in the Fig. 14. The reaction rate was found to be reduced sharply when CO was introduced into the gas phase during the oxidation. In the presence of CO, the reaction was first order in CO and zero order in O_2. The CO molecule retained its integrity during the oxidation reaction [65].

The number of CO_2 molecules adsorbed corresponded to the number of oxygen atoms pre-adsorbed on the surfaces of catalyst. The equivalent concentration of oxygen atoms in the gas phase and on the surface, therefore, heterogeneous exchange reaction was taking places. The mechanisms of CO oxidation on the surfaces of catalysts are a top tactic in

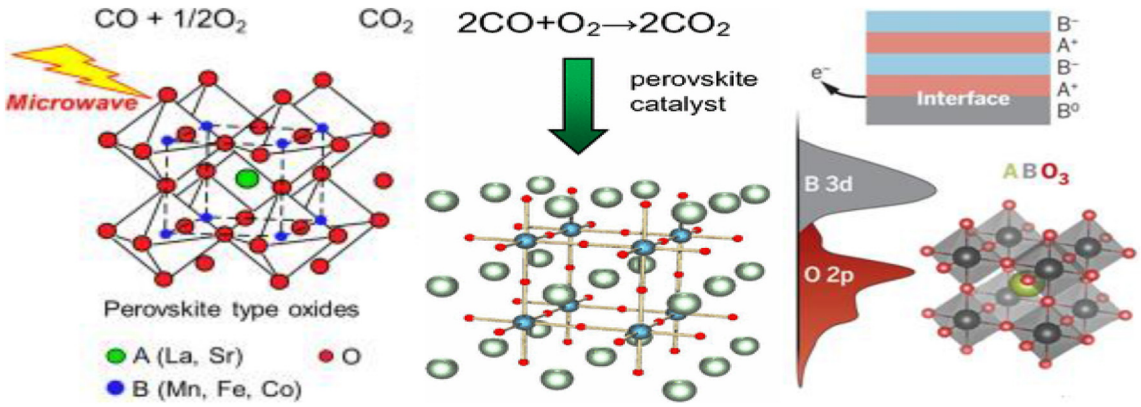

Fig. 12. Reaction mechanism of perovskite catalysts [33,34,42–44].

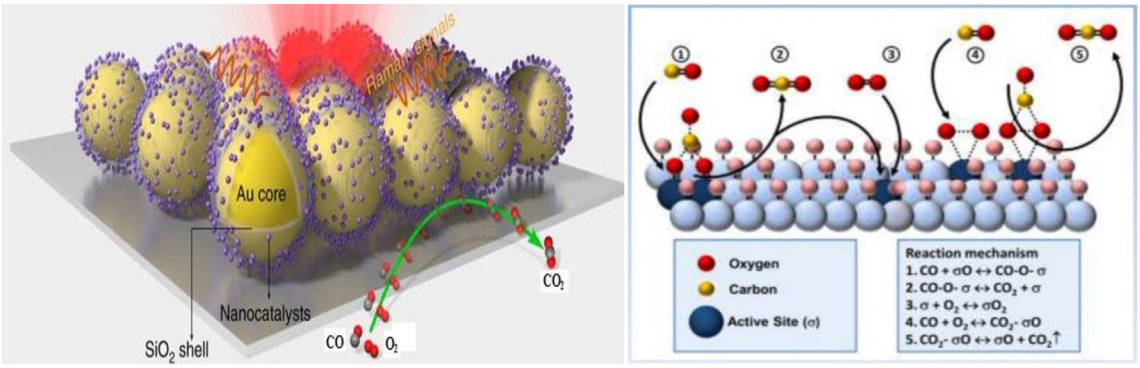

Fig. 13. Marsvan Krevelen mechanism for conversion of carbon monoxide [27,28,31,32].

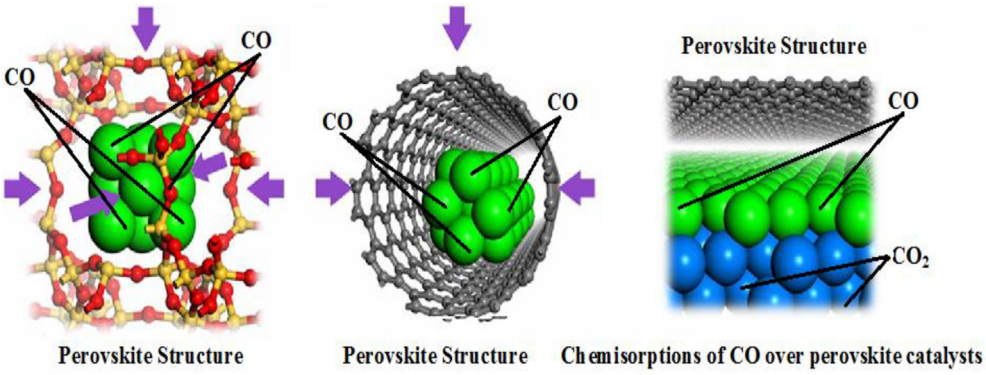

Fig. 14. Mechanism for CO conversions over perovskite catalysts [56–58,70–72].

nature, therefore the reversible failure and uptake of huge oxygen or for the production and destruction of vacancies reported these systems as attractive oxidation catalysts. The inconsistent oxygen in the perovskite structure is accountable for the unusual performance of these materials. The removal of oxygen from frame works of perovskite structure and possibility of deriving different structural in ideal perovskites catalysts [67–70]. The various mechanisms of CO oxidation and formation of CO_2 over perovskite catalysts are shown in the Fig. 14.

The mixing of the pollutants gases are constantly measured by an oxygen sensor and the air-to-fuel ratio is tuned consequently by the fuel-control reaction conditions. The kinetics study of CO oxidation over perovskite catalysts at the adsorption and desorption cycle is shown in the Fig. 15. The performance of perovskite-type oxides convincingly increases with increasing the concentration of available active phase. Therefore the higher performance was obtained on extruded and layered on the structured catalysts containing a more adding of energetic component [71,72].

5. Deactivation of perovskites catalysts

The activity and selectivity of perovskites catalysts in catalytic converter are crucial for CO oxidation reaction. The catalyst deactivation can be divided into six different types: (i) poisoning, (ii) thermal degradation, (iii) fouling, (iv) vapor compound formation (v) vapor-solid reactions and (vi) crushing/abrasion. The lead, sulphur poisoning, carbon formation and sintering is the main cause of catalyst deactivation. The dispersion of active phase rapidly decreases, which is one of the main reason for catalyst deactivation. The catalytic activity of metal support (La_2O_3) is susceptible to sulphur poisoning, which is one of the most contaminants in catalytic converter exhaust emissions. The substitutions

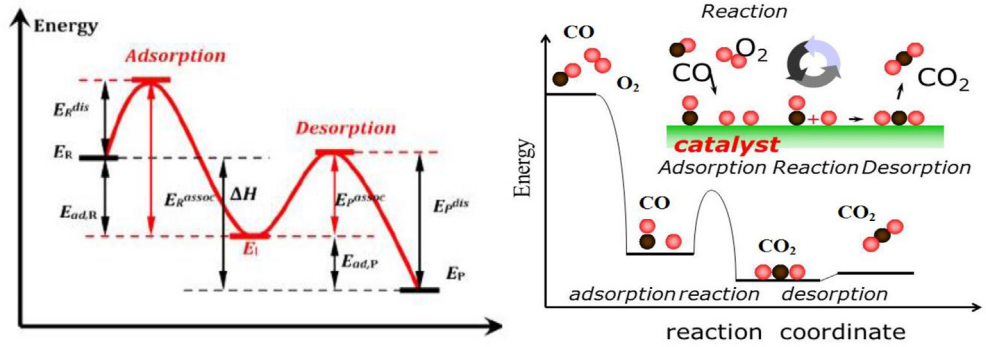

Fig. 15. Kinetics analysis of CO oxidations over perovskite catalysts [43,44,50–52].

of materials in perovskite catalysts should not influence their activity in reforming reaction; but the changes in structure should remain their resistance to carbon deposition as well as to sulphur poisoning [66]. The promising stability of this catalyst could be attributed to the high mobility of oxygen on the interface between the MnCeOx solid solution and MnOx, which is critical for removing the Cl species produced during CB decomposition. The Ce–Pr mixed oxides, specifically $Ce_{0.5}Pr_{0.5}O_2$, have been reported to exhibit higher stability for the catalytic combustion of 1,2-dichloroethane. Conspicuous catalytic deactivation was, however, induced through the formation of by-products such as C–C coupling products, higher chlorinated compounds and cracking compounds. The sulphur poisoning over perovskite catalysts are shown in the Fig. 16. The $LaMnO_3$ perovskite oxide catalyst synthesized by co-precipitation was found to exhibit significant activity for the catalytic oxidation of CO emissions. Moreover, its activity was enhanced by A or B site substitution. Because a promising catalyst for industrial applications should present not only high catalytic activity, but also good stability and durability, further study relative to stability and deactivation issues for $LaMnO_3$ is now of the utmost urgency and significance [73,74].

The stability of perovskite catalyst could be well recognized to the high mobility of oxygen on the interface of mixed oxides. The dispersion of active phase rapidly decreases, which is one of the main reasons for catalyst deactivation. Chemical poisoning and coke formation are one of the main reasons for catalytic deactivation. The deactivation of perovskite catalyst reduced the surface area of catalysts if available to the surroundings [75,76].

The poisoning is due to strong adsorption of feed impurities; therefore, the poisoned catalysts are generally difficult to regenerate. Catalyst restoration is the least desirable approach to defeat catalyst deactivation and restore their activity and selectivity. The catalyst regeneration and reforming processes are mostly classified into three types: semi-regenerative, cyclic and constant regenerative process. Catalyst regeneration is mainly to recover activity defeat due to fast coking with failure of active metal diffusion. The regeneration of perovskite catalysts by various processes is shown in the Fig. 17. The small amounts of noble metals added in perovskite due to their regenerating mechanism. The Pd in $LaFe_{0.95}Pd_{0.05}O_3$ exists as a solid solution dispersed all over perovskite lattice. In the perovskite catalyst, the oxidizing/reducing cycle maintains the catalytic activity by regenerating the nano-particles and preventing metal nano-particle growth [77,78].

6. Challenges and future applications of perovskite catalysts

Perovskite oxides are versatile materials due to their wide variety of compositions offering promising catalytic properties, especially in oxidation reactions. Perovskites ABO_3 are exciting materials for oxidation catalysis as they provide considerable flexibility regarding their compositions and the possibility to implement oxygen vacancies with a selective modification of the cationic sublattice An interesting property of perovskite nanocrystals is their ability to undergo reversible exchange of halide ions (I, Br and Cl). While this property is useful in preparing nanocrystals of different halide composition, it also hinders the use of different nanocrystals or films. Upon contact, two different nanocrystals (e.g., $CsPbBr_3$ and $CsPbI_3$) form mixed halide perovskites. Another interesting approach is to couple perovskite nanocrystals with a different semiconductor to create a hetero structure with Type I or Type II configurations, based on their bandgap alignment. Furthermore, the perovskite structure is tolerant to the formation of anionic and cationic vacancies, which can tune the catalytic properties of the materials. The oxygen activation and dissociation capabilities at perovskite surfaces are strongly correlated to the composition and number of oxygen vacancies. These vacancies can promote the formation of monoatomic oxygen (O^-), which would act as the primary type of oxygen in the system. One straightforward approach to determine catalytic activity and oxygen activation capability is the CO oxidation reaction as a prototypical reaction for heterogeneous processes. The reaction only has a single gaseous product, which interacts with metal

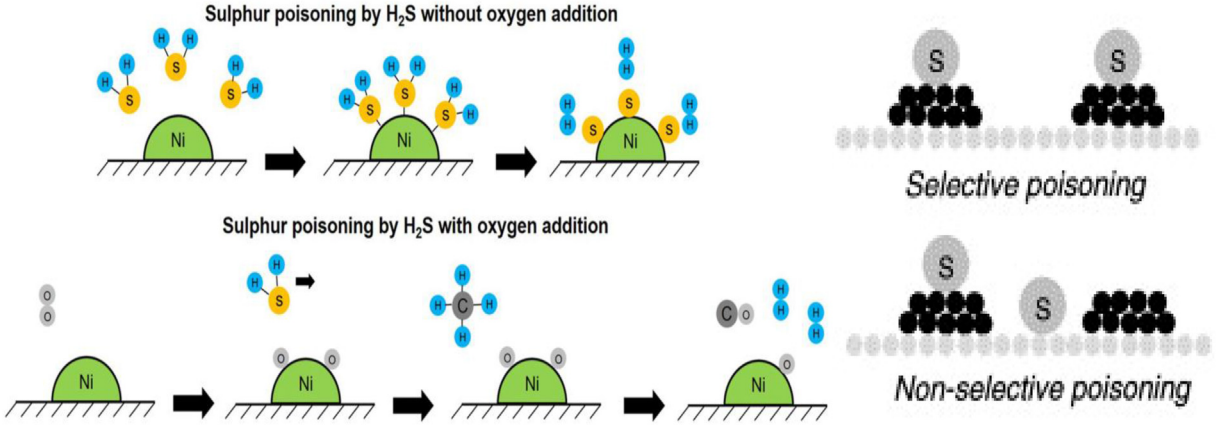

Fig. 16. Sulphur poisoning in the various perovskite catalysts [61,62,67,68].

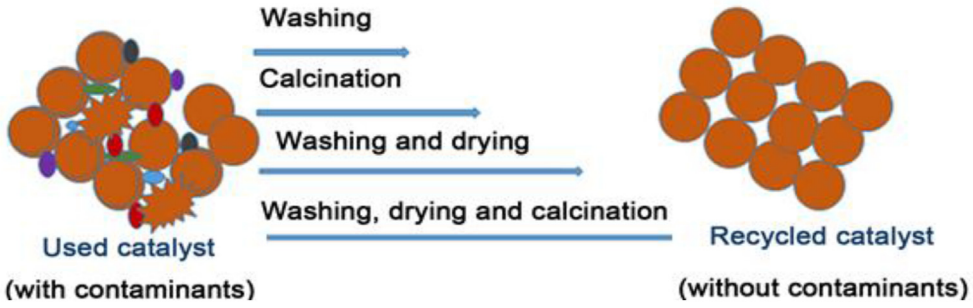

Fig. 17. Regeneration of perovskite catalysts [71,72].

oxides either strongly or weakly. For Co_3O_4, no adsorption of CO_2 on the surface was found, whereas an adsorption capacity has been reported for Al_2O_3. Furthermore, this reaction pathway is involved in the total oxidation mechanism of hydrocarbons and oxygenated molecules, which leads to a decrease in selectivity towards valuable intermediates. The effect of Co incorporation into oxides and $LaFeO_3$ perovskite on CO oxidation catalysis has also attracted attention. For example, including only 1% Co has been shown to increase the CO oxidation activity of NiO significantly, but no steady conversion increase with Co incorporation has been observed. On Sr and Co-doped $LaFeO_3$, highly at intermediate Co level were observed for transition metal surface content, oxygen storage capacity, reducibility and methanol oxidation activity. In our upcoming research work, we will perform further mechanistic studies on the CO oxidation on different perovskites catalysts and also test the performances in different oxidation reactions.

7. Conclusions

In perovskite catalysts the partial substitution of cations, which stabilizes unusual oxidation states of metal components and creates anionic or cationic vacancies within the perovskite lattice. The partial substitution of cations can increase the reducibility and metal dispersion of catalyst. The support perovskites on porous materials like a monolith or a usual high surface area material to raising the amount of uncovered perovskite active sites. The reaction intermediates and a mechanistic condition are paramount for fundamental insight into the origin of activity and product selectivity. Structure-function relationships are crucial concept to develop basic guidelines for the design of more active catalysts after the mechanism is sufficiently understood. The surface area of perovskite oxides falls behind into simple metals. In addition, organometallic halide perovskites exhibited efficient intrinsic properties to be utilized as a photovoltaic solar cell with good stability and high efficiency. The reducing of particle size, making perovskites with hierarchical porosity is a promising approach to enhance mass activity and control applications. Nano-perovskites have been utilized as catalysts in oxygen reduction and hydrogen evolution reactions exhibiting high electro-catalytic activity, lower activation energy and high electron transfer kinetics. In addition, some perovskites are promising candidates for the development of effective anodic catalysts for direct fuel cells showing better catalytic performance. The relative ease of preparation, thermal and chemical stability and good catalytic activities of perovskites catalysts offer good performances for environmental pollution.

Funding statement

This research received no specific grant from any funding agency in the public, commercial, or not-for-profit sectors.

Data availability statement

The statements in the paper are properly cited in the manuscript and no additional data is available.

Declaration of competing interest

The authors declare no conflict of interest.

Acknowledgements

The authors are thankful for the support from all the faculty members and lab in charges of Environmental Engineering Department, Rajiv Gandhi Proudyogiki Vishwavidyalaya, Bhopal, India.

References

[1] J.L. Hueso, D. Martínez-Martínez, A. Caballero, A.R. González-Elipe, B.S. Mun, M. Salmerón, Near-ambient X-ray photoemission spectroscopy and kinetic approach to the mechanism of carbon monoxide oxidation over lanthanum substituted cobaltites, Catal Commun 10 (2009) 1898–1902.
[2] A. Mishra, R. Prasad, Preparation and application of perovskite catalysts for diesel soot emissions control: an overview, Catal Rev Sci Eng 56 (1) (2014) 57–86.
[3] P.D. Petrolekas, I.S. metcalfe, The study of La(Sr)MnO_3 catalyst during carbon monoxide oxidation, J Catal 152 (1994) 147–163.
[4] W. Liu, Flytzani-Stephanopoulos, Transition metal-promoted oxidation catalysis by fluorite oxides: a study of CO oxidation over Cu-CeO_2, Chem Eng J 64 (1996) 283–294.
[5] V. Blasin-Aubé, J. Belkouch, L. Monceaux, General study of catalytic oxidation of various VOCs over $La_{0.8}Sr_{0.2}MnO_{3+x}$ perovskite catalyst—influence of mixture, Appl Catal B Environ 43 (2003) 175–186.
[6] J. Shu, S. Kaliaguine, Well-dispersed perovskite-type oxidation catalysts, Appl Catal B Environ 16 (1998) 303–308.
[7] N. Mizuno, M. Tanaka, M. Misono, Reaction between carbon monoxide and Perovskite-type mixed oxides, J Chem Soc Faraday Trans 88 (1992) 91–95.
[8] S. Shen, H. Weng, Comparative study of catalytic reduction of carbon monoxide over the $La_{1-x}SrxBO_3$ (B = Mn, Fe, Co, Ni) Catalysts, Ind Eng Chem Res 37 (1998) 2654–2661.
[9] S. Chand, A.K. Sharma, A. Garg, M. Mishra, Supported perovskites as catalysts for CO oxidations, J Sci Ind Res 59 (2000) 944–948.
[10] K. Wang, P. Zhong, A kinetic study of CO oxidation over the perovskite-like oxide $LaSrNiO_4$, J Serb Chem Soc 75 (2) (2010) 249–258.
[11] F. Patel, S. Patel, $La_{1-X}Sr_XCoO_3$ (X=0, 0.2) perovskites type catalyst for carbon monoxide emission control from auto-exhaust, vol. 51, Procedia Engineering of 3rd Nirma University International Conference, 2013, pp. 324–329.
[12] H. Yasuda, Y. Fujiwara, N. Mizuno, M. Misono, Oxidation of carbon monoxide on $LaMn_{1-X}Cu_XO_3$, perovskite-type mixed oxides, J Chem Soc Faraday Trans 90 (1994) 1183–1189.
[13] S. Jaenicke, G.K. Chuah, J.Y. Lee, Catalytic CO oxidation over manganese containing perovskites, Journal of Environmental Monitoring and Assessment 19 (1991) 131–138.
[14] M. Abdolrahmani, M. Parvari, M. Habibpoor, Effect of copper substitution and preparation methods on the $LaMnO_{3+\S}$ structure and catalysis of methane combustion and CO oxidation, Chin J Catal 31 (2010) 394–403.
[15] T. Hayakawa, A.G. Andersen, M. Shimizu, K. Suzuki, K. Takehira, Partial oxidation of carbon monoxide to synthesis gas over some titanates based perovskite oxides, Catal Lett 22 (1993) 307–317.
[16] F. Teng, S. Liang, M. Gaugeu, R. Zong, W. Yao, Y. Zhu, Carbon nanotubes-templated assembly of $LaCoO_3$ nanowires at low temperatures and its excellent catalytic properties for CO oxidation, Catal Commun 8 (2007) 1748–1754.
[17] J. Asgardi, J.C. Calderon, F. Alcaide, A. Querejeta, L. Calvillo, M. Lazaro, G. Garcia, E. Pastor, Carbon monoxide and ethanol oxidation of PtSn supported catalysts: effect of the nature of the carbon supported and Pt:Sn composition, Appl Catal B Environ 169 (2015) 33–41.
[18] P. Doggali, Y. Teraoka, S. Rayalu, S. Labhsetwar, Effect of A-site substitution in perovskites: catalytic properties of $PrMnO_3$ and Ba/K/Ce substituted $PrMnO_3$ for CO and PM oxidation, J Environ Chem Eng 3 (2015) 420–428.
[19] L. Jian, W. Jiqiu, Z. Zhen, X. Chunming, W. Yuechang, D. Aijun, J. Guiyan, Synthesis of $La_XK_{1-X}CoO_3$ nanorod and their catalytic performances for CO oxidation, J Rare Earths 32 (2014) 170–175.

[20] S. Dey, G.C. Dhal, D. Mohan, R. Prasad, Kinetics of catalytic oxidation of carbon monoxide over CuMnAgOx Catalyst, Materials Discovery 8 (2017) 18–25.
[21] R.G. Shetkar, A.V. Salker, Solid state and catalytic CO oxidation studies on $Zn_{1-X}Ni_XMnO_3$ system, Mater Chem Phys 108 (2008) 435–439.
[22] X. Yan, Q. Huang, B. Li, X. Xu, Y. Chen, S. Zhu, S. Shen, Catalytic performance of $LaCo_{0.5}M_{0.5}O_3$ (M = Mn, Cr, Fe, Ni, Cu) perovskite-type oxides and $LaCo_{0.5}Mn_{0.5}O_3$ supported on cordierite for CO oxidation, J Ind Eng Chem 19 (2013) 561–565.
[23] Y. Zhang-Steenwinkel, J. Beckers, A. Bliek, Surface properties and catalytic performance in CO oxidation of cerium substituted lanthanum–manganese oxides, Appl Catal Gen 235 (2002) 79–92.
[24] P. Doggali, S. Kusaba, Y. Teraoka, P. Chankapure, S. Rayalu, N. Labhsetwar, $La_{0.9}Ba_{0.1}CoO_3$ perovskite type catalysts for the control of CO and PM emissions, Catal Commun 11 (2010) 665–669.
[25] S. Dey, G.C. Dhal, D. Mohan, R. Prasad, Low-temperature complete oxidation of CO over various manganese oxide catalysts, Atmos Pollut Res 9 (2018) 755–763.
[26] B. Gao, J. Deng, Y. Liu, Z. Zhao, X. Li, Y. Wang, H. Dai, Mesoporous $LaFeO_3$ catalysts for the oxidation of toluene and carbon monoxide, Chin J Catal 34 (2013) 2223–2229.
[27] S. Dey, G.C. Dhal, D. Mohan, R. Prasad, Effect of preparation conditions on the catalytic activity of CuMnOx catalysts for CO Oxidation, Bull Chem React Eng Catal 12 (3) (2017) 1–15.
[28] S. Dey, G.C. Dhal, D. Mohan, R. Prasad, Characterization and activity of CuMnOx/γ-Al_2O_3 catalyst for oxidation of carbon monoxide, Materials Discovery 8 (2017) 26–34.
[29] S. Dey, G.C. Dhal, D. Mohan, R. Prasad, Copper based mixed oxide catalysts (CuMnCe, CuMnCo and CuCeZr) for the oxidation of CO at low temperature, Material Discovery 10 (2017) 1–14.
[30] H. Einaga, Y. Nasu, M. Oda, H. Saito, Catalytic performances of perovskite oxides for CO oxidation under microwave irradiation, Chem Eng J 283 (2016) 97–104.
[31] A. Gholizadeh, A. Malekzadeh, M. Ghiasi, Structural and magnetic features of $La_{0.7}Sr_{0.3}$ $Mn_{1-X}Co_XO_3$ nanocatalysts for ethane combustion and CO oxidation, Ceram Int 42 (2016) 5707–5717.
[32] C.A. Chagas, E.F. De-Souza, R.L. Manfro, S.M. Landi, M.M.V.M. Souza, M. Schmal, Copper as promoter of the NiO-CeO_2 catalyst in the preferential CO oxidation, Appl Catal B Environ 182 (2016) 257–265.
[33] F. Teng, B. Gaugeu, S. Liang, Y. Zhu, Preparation of $LaSrCuO_4$ naowires by carbon nanotubes and their catalytic and chemilumine scence properties for CO oxidation, Appl Catal Gen 328 (2007) 156–162.
[34] R.T. Dong, H.L. Wang, Q. Zhang, X.T. Xu, F. Wang, B. Li, Shape-controlled synthesis of Mn_2O_3 hollow structures and their catalytic properties, CrystEngComm 17 (2015) 7406–7413.
[35] F.S. Toniolo, M. Schmal, Improvement of catalytic performance of perovskites by partial substitution of cations and supporting on high surface area materials, Chapter 18 (2016), https://doi.org/10.5772/61279. Intech Open Science.
[36] B. Kucharczyk, Catalytic oxidation of carbon monoxide on Pd-containing $LaMnO_3$ perovskites, Catal Lett 145 (16) (2015) 1237–1245.
[37] S. Dey, G.C. Dhal, D. Mohan, R. Prasad, Synthesis and characterization of $AgCoO_2$ catalyst for oxidation of CO at a low temperature, Polyhedron 155 (2018) 102–113.
[38] N.F. Atta, A. Galal, E.H. El-Ads, Perovskite nanomaterials – synthesis, characterization, and applications, Intech Open, 2015, pp. 107–151.
[39] S. Dey, G.C. Dhal, D. Mohan, R. Prasad, Study of Hopcalite (CuMnOx) catalysts prepared through a novel route for the oxidation of carbon monoxide at low temperature, Bull Chem React Eng Catal 12 (3) (2017) 393–407.
[40] F. Sani, S. Shafie, H.N. Lim, A.O. Musa, Advancement on lead-free organic-inorganic halide perovskite solar cells: a review, Mater Rev 11 (6) (2018) 1008.
[41] E. Meyer, D. Mutukwa, N. Zingwe, R. Taziwa, Lead-free halide double perovskites: a review of the structural, optical and stability properties as well as their viability to replace lead halide perovskites, Mater Rev 8 (2018) 667.
[42] R.S. Roth, Classification of perovskite and other ABO_3-type compounds, J Res Natl Bur Stand 58 (2) (1957) 2736.
[43] M. Risch, Perovskite electro catalysts for the oxygen reduction reaction in alkaline media, Catalysts 154 (7) (2017) 1–31.
[44] I. Yamada, Novel catalytic properties of quadruple perovskites, Sci Technol Adv Mater 18 (1) (2017) 541–548.
[45] S.I. Suárez-Vázquez, A. Cruz-López, C.E. Molina-Guerrero, A.I. Sánchez-Vázquez, C. Macías-Sotelo, Effect of dopant loading on the structural and catalytic properties of Mn-doped $SrTiO_3$ catalysts for catalytic soot combustion, Catalysts 8 (71) (2018) 1–11.
[46] S. Dey, G.C. Dhal, D. Mohan, R. Prasad, The choice of precursors in the synthesizing of CuMnOx catalysts for maximizing CO oxidation, Int J Integrated Care 9 (2018) 199–214.
[47] B. Viswanathan, CO oxidation and NO reduction on perovskite oxides, Catalyis Reviews 34 (4) (1992) 337–354.
[48] P.R. Zonouz, M.E. Masoumi, A. Niaei, A. Tarjomannejad, Experimental and kinetic study of CO oxidation over $LaFe_{1-X}Cu_xO_3$ (x=0, 0.2, 0.4, 0.6) perovskite-type oxides, Iranian Journal of Chemical Engineering 15 (2) (2018) 91–102.
[49] Y. Yi, P. Zhang, Z. Qin, C. Yu, W. Li, Q. Qin, B. Li, M. Fan, X. Liang, L. Dong, Low temperature CO oxidation catalysed by flower-like Ni–Co–O: how physicochemical properties influence catalytic performance, RSC Adv 8 (2018) 7110–7122.
[50] J. Zhu, Z. Zhao, D. Xiao, J. Li, X. Yang, Y. Wu, CO oxidation, NO decomposition, and NO + CO reduction over perovskite-like oxides La_2CuO_4 and $La_{2-X}Sr_XCuO_4$: an MS-TPD study, Ind Eng Chem Res 44 (12) (2005) 4227–4233.
[51] I. Kocemba, J. Długołecka, M. Wrobel-JeÌdrzejewska, J. Rogowski, I. Dobrosz-Gomez, J. Rynkowski, React Kinet Mech Catal 123 (2018) 659–677.
[52] Y. Liu, H. Dai, Y. Du, J. Deng, L. Zhang, Z. Zao, C.T. Au, Controlled preparation and high catalytic performance of three-dimensionally ordered macroporous $LaMnO_3$ with nanovoid skeletons for the combustion of toluene, J Catal 287 (2012) 149–160.
[53] X. Lin, S. Li, H. He, Z. Wu, J. Wu, L. Chen, D. Ye, Evolution of oxygen vacancies in MnOx-CeO_2 mixed oxides for soot oxidation, Appl Catal B 223 (2018) 91–102.
[54] C. Lee, Y. Jeon, S. Hata, J. Park, R. Akiyoshi, H. Saito, Y. Teraoka, Y. Shul, H. Einaga, Three-dimensional arrangements of perovskite-type oxide nano-fiber webs for effective soot oxidation, Appl Catal B 191 (2016) 157–164.
[55] L. Zhang, Y. Nie, C. Hu, J. Qu, Enhanced fenton degradation of rhodamine B over nanoscaled Cu-doped $LaTiO_3$ perovskite, J. Appl. Catal. B 125 (2012) 418–424.
[56] A. Grimaud, W.T. Hong, Y. Shao-Horn, J.M. Tarascon, Anionic redox processes for electrochemical devices, Nat Mater 15 (2016) 121–126.
[57] C. Yang, A. Grimaud, Factors controlling the redox activity of oxygen in perovskites: from theory to application for catalytic reactions, Catalysts 7 (2017) 149.
[58] M. Komo, A. Hagiwara, S. Taminato, M. Hirayama, R. Kanno, Oxygen evolution and reduction reactions on $La_{0.8}Sr_{0.2}CoO_3$ (001), (110) and (111) surfaces in an alkaline solution, Electrochemistry 80 (2012) 834–838.
[59] J. Gallego, C. Batiot-Dupeyrat, J. Barrault, F. Mondragon, Severe deactivation of a $LaNiO_3$ perovskite-type catalyst precursor with H_2S during methane dry reforming, Energy Fuels 23 (2009) 4883–4886.
[60] P.K. Vagholkar, Self regenerating catalysts: platinum group metal perovskite catalysts, Int J Sci Res 4 (11) (2015) 352–355.
[61] J.R. Petrie, V.R. Cooper, J.W. Freeland, T.L. Meyer, Z. Zhang, D.A. Lutterman, H.N. Lee, Enhanced bifunctional oxygen catalysis in strained $LaNiO_3$ perovskites, J Am Chem Soc 138 (2016) 2488–2491.
[62] W.S. Kim, G. Anoop, H.J. Lee, S.S. Lee, J.H. Kwak, H.J. Lee, J.Y. Jo, Facile synthesis of perovskite $LaMnO_{3+\delta}$ nanoparticles for the oxygen reduction reaction, J Catal 344 (2016) 578–582.
[63] P.C.K. Vesborg, T.F. Jaramillo, Addressing the terawatt challenge: scalability in the supply of chemical elements for renewable energy, RSC Adv 2 (2012) 7933–7947.
[64] Z. Zeng, F. Calle-Vallejo, M.B. Mogensen, J. Rossmeisl, Generalized trends in the formation energies of perovskite oxides, Phys Chem Chem Phys 15 (2013) 7526–7533.
[65] S. Dey, G.C. Dhal, D. Mohan, R. Prasad, Synthesis of silver promoted CuMnOx catalyst for ambient temperature oxidation of carbon monoxide, J Sci: Advanced Materials and Devices (2019) 1–10.
[66] P. Avila, M. Montes, E.E. Mir, Monolithic reactors for environmental applications: a review on preparation technologies, Chem Eng J 109 (2005) 11–36.
[67] S. Royer, F. Berube, S. Kaliaguine, Effect of the synthesis conditions on the redox and catalytic properties in oxidation reactions of $LaCo_{1-X}FexO_3$, Appl Catal, A 282 (2005) 273–284.
[68] N.K. Labhsetwar, A. Watanabe, T. Mitsuhashi, New improved syntheses of $LaRuO_3$ perovskites and their applications in environmental catalysis, Appl Catal B 40 (2003) 21–30.
[69] Y. Liu, H. Zheng, J. Liu, T. Zhang, Preparation of high surface area $La_{1-X}AxMnO_3$ (A = Ba, Sr or Ca) ultra-fine particles used for CH_4 oxidation, Chem Eng J 89 (2002) 213–221.
[70] H.X. Dai, C.F. Ng, C.T. Au, Perovskite-type Halo-oxide $La_{1-x}SrxFeO_{3-\delta}X\sigma$ (X = F, Cl) catalysts selective for the oxidation of ethane to ethene, J Catal 189 (2000) 52–62.
[71] S. Dey, G.C. Dhal, D. Mohan, R. Prasad, Synthesis of highly active cobalt catalysts for low temperature CO oxidation, Chemical Data Collections 24 (2019), 100283.
[72] S. Dey, G.C. Dhal, D. Mohan, R. Prasad, Application of hopcalite catalyst for controlling carbon monoxide emission at cold-start emission conditions, J Traffic Transport Eng 6 (5) (2019) 419–440.
[73] M. Muhler, R. Schlogl, G. Ertl, The nature of the iron oxide-based catalyst for dehydrogenation of ethylbenzene to styrene, J Catal 138 (1992) 413–444.
[74] S. Dey, G.C. Dhal, D. Mohan, R. Prasad, Ambient temperature complete oxidations of carbon monoxide using hopcalite catalysts for fire escape mask applications, Advanced Composites and Hybrid Materials (2019) 1–19, https://doi.org/10.1007/s42114-019-00108-5.
[75] X. Zhang, F. Hou, H. Li, Y. Yang, Y. Wang, N. Liu, Y. Yang, A strawsheave-like metal organic framework Ce-BTC derivative containing high specific surface area for improving the catalytic activity of CO oxidation reaction, Microporous Mesoporous Mater 259 (2018) 211–219.
[76] Y. Shi, Y. Zhou, Y. Lou, Z. Chen, H. Xiong, Y. Zhu, Homogeneity of supported single-atom active sites boosting the selective catalytic transformations, Adv Sci (2022) 1–40, 2201520.
[77] L. Dai, X.B. Lu, G.H. Chu, C.H. He, W.C. Zhan, G.J. Zhou, Surface tuning of $LaCoO_3$ perovskite by acid etching to enhance its catalytic performance, Rare Met 40 (2021) 555–562.
[78] Z. Zhu, W. Guo, Y. Zhang, C. Pan, J. Xu, Y. Zhu, Y. Lou, Research progress on methane conversion coupling photo catalysis and thermo catalysis, Carbon Energy 3 (2021) 519–540.